applied sciences

MDPI

Article

Application of Random Forest Algorithm in Estimating Dynamic Mechanical Behaviors of Reinforced Concrete Column Members

Rou-Han Li *, Mao-Yuan Li, Xiang-Yang Zhu and Xiang-Wei Zeng

Department of Civil Engineering, College of Transportation Engineering, Dalian Maritime University, Dalian 116026, China; limaoyuan@dlmu.edu.cn (M.-Y.L.); zhuxiangyang@dlmu.edu.cn (X.-Y.Z.); zxw1120221644@dlmu.edu.cn (X.-W.Z.)

* Correspondence: lirouhan@dlmu.edu.cn

Abstract: In this paper, an innovative method is put forward for estimating the dynamic mechanical behaviors of reinforced concrete (RC) column members by applying the random forest algorithm. Firstly, the development of dynamic modified coefficient (*DMC*) predictive models and the realization of the proposed method were elaborated. Then, due to the lack of dynamic loading tests on RC column members, a numerical model of RC columns considering the dynamic modification on flexural, shear and bond-slip behaviors was developed on the OpenSees platform, and the model accuracy and the effectiveness were verified with the available test results. Moreover, by comparing the simulated results of the hysteretic curve using numerical models with different complexities, the influences of dynamic modification and the deformation sub-element were investigated. Furthermore, a numerical experiment database was established to obtain the training data for developing the *DMC* predictive models of critical mechanical behavior parameters, including the yielding bearing capacity, ultimate bearing capacity and displacement ductility. Finally, the results of feature importance for different input parameters were studied, and the model accuracy was evaluated using the test set and available experimental data. It was revealed that the predictive models developed using the random forest algorithm can be employed to reliably estimate the dynamic mechanical behaviors of RC column members.

Keywords: dynamic mechanical behavior; reinforced concrete column; random forest algorithm; dynamic modified coefficient; predictive model

check for updates

Citation: Li, R.-H.; Li, M.-Y.; Zhu, X.-Y.; Zeng, X.-W. Application of Random Forest Algorithm in Estimating Dynamic Mechanical Behaviors of Reinforced Concrete Column Members. *Appl. Sci.* **2024**, *14*, 2546. https://doi.org/10.3390/app14062546

Academic Editor: Syed Minhaj Saleem Kazmi

Received: 2 February 2024
Revised: 9 March 2024
Accepted: 15 March 2024
Published: 18 March 2024

Copyright: © 2024 by the authors. Licensee MDPI, Basel, Switzerland. This article is an open access article distributed under the terms and conditions of the Creative Commons Attribution (CC BY) license (https://creativecommons.org/licenses/by/4.0/).

1. Introduction

Reinforced concrete (RC) columns are critical load-bearing components in building structures. Accurately and reliably evaluating their mechanical behaviors under dynamic loading is of great importance in the seismic design and analysis of RC structures. It is widely known that RC materials are strain-rate sensitive, meaning that the properties of reinforcement and concrete under various loading rates are quite different [1–3]. As a result, different mechanical behaviors of RC columns have been measured under dynamic loading and quasi-static loading [4–7]. Generally, the available dynamic loading tests on RC columns indicate that the bearing capacity and stiffness, as well as the energy dissipation capacity, are increased while the ductility might be decreased and the performance deterioration is aggravated for RC columns under relatively high loading rates [8].

Quite a number of research works have been carried out to test the dynamic mechanical behaviors of RC columns. Among them, the experimental method [9] is the most convincing; however, the test data are limited due to the large financial and human costs. As an alternative, some scholars have made attempts to establish numerical models to simulate the dynamic mechanical behaviors of structural members [10–13] and further develop empirical models of dynamic increase factor (DIF) to estimate the critical mechanical behavior parameters [14–17]. Based on the dynamic loading test results and the Bayesian

updating method, Li et al. [18] developed predictive models of the dynamic modified coefficient (*DMC*) for RC columns, which can be used to estimate the dynamic mechanical behaviors of RC columns under seismic loading. The disadvantages of available studies can be summarized as: (1) the predictive models of DIF at the member level were established on limited experimental or numerical data, and (2) the numerical models are not sufficiently accurate because the dynamic effect on the shear and bond-slip behaviors of RC column members have often been neglected.

With the rapid development of data science and computer technology, machine learning has been widely applied to the field of structural engineering in recent years [19–22]. Many machine learning techniques have been adopted by researchers to predict the mechanical behaviors and failure mode of RC structural members [23–25]. The empirical-based support vector machine method was employed by Liu et al. [26] to predict the force-deformation backbone with the basic structural parameters of RC columns taken as the inputs. Todorov et al. [27] used different machine learning methods to identify different damage states, such as spalling, core crushing and bar buckling of RC bridge piers, and the accuracy of the machine learning-based models was improved as compared with the existing physics-based empirical models. Luo et al. [28] proposed a machine learning-based backbone curve model of force-deformation for flexure- and shear-critical columns, and its robustness and accuracy were demonstrated by comparison with the traditional modeling approaches. By employing ensemble machine learning techniques, Feng et al. [29] studied the failure mode classification and bearing capacity prediction of RC columns. Their proposed method had better performance than the single learning method and the empirical formulas provided by the design codes.

For this paper, predictive models of the dynamic modified coefficient (*DMC*) were developed for estimating the dynamic mechanical behaviors of RC columns through machine learning (i.e., the random forest algorithm). In Section 2, the random forest method is introduced for developing *DMC* predictive models. In Section 3, a numerical model of RC columns considering the dynamic effect is established and validated. Moreover, a numerical database for model training in terms of critical mechanical behavior parameters of RC columns is developed. In Section 4, the feature importance and the model accuracy are evaluated using the testing set data. Finally, in Section 5, the main conclusions of this paper are summarized and further works are also proposed.

2. Method for Estimating Dynamic Mechanical Behaviors of RC Columns

2.1. Predictive Models of Dynamic Modified Coefficient

The results of available experiments on RC columns indicate that with the increase of the loading rate, the bearing capacity is enhanced while the ductility is likely to be reduced [6,7]. Similar to the widely used empirical models of dynamic increase factor (DIF) [30–32], which were established at the material level, the dynamic modified coefficient is defined as the ratio of the mechanical behavior parameter under the dynamic loading rate (denoted by the subscript 'd') to the corresponding value under static loading rate (denoted by the subscript 's'). In this paper, the predictive models of *DMC* for the yielding bearing capacity F_y, the ultimate bearing capacity F_u and the ductility coefficient μ are expressed as

$$DMC_{F_y}(input_1, input_2, \cdots, input_n) = F_{yd}/F_{ys} \quad (1)$$

$$DMC_{F_u}(input_1, input_2, \cdots, input_n) = F_{ud}/F_{us} \quad (2)$$

$$DMC_{\mu}(input_1, input_2, \cdots, input_n) = \mu_d/\mu_s \quad (3)$$

where $input_1$, $input_2$, …, $input_n$ denote the input variables that have a considerable influence on the mechanical behavior and dynamic effect of RC columns. Based on the available experimental observations, 5 structural design parameters of RC column members, including the axial load ratio (n_0), shear span ratio (λ), strength of longitudinal reinforcement (f_y), compressive strength of concrete (f_c') and stirrup spacing (S) are selected as input

variables. Moreover, a loading rate related parameter, i.e., the strain rate index (*SRI*) [33], is incorporated into the predictive models, which is defined as

$$SRI = \lg(\dot{\varepsilon}_d / \dot{\varepsilon}_0) \quad (4)$$

where $\dot{\varepsilon}_d$ and $\dot{\varepsilon}_0$ denote the dynamic and quasi-static strain rates, respectively, and the quasi-static strain rate is taken as 1×10^{-5}/s [18].

Due to the inadequacy of dynamic loading test data on RC columns, this paper develops the predictive models of *DMC* based on the numerical results of mechanical behavior parameters of RC columns. To ensure the accuracy and reliability of predictive models, it is noted that the numerical simulation needs to sufficiently consider the influence of the dynamic effect on the mechanical behavior and deformation mechanism of RC columns under different loading rates. More importantly, a large number of training data are required in the model development when employing the random forest method.

2.2. Random Forest Method

The traditional method for estimating the mechanical behaviors of RC columns is by conventional regression fitting with the experimental or numerical data. In this paper, the random forest method is employed to develop predictive models for rapidly estimating the dynamic modified coefficient (*DMC*) of RC columns. As one of the commonly used machine learning techniques, the random forest method has been applied in solving various problems in the field of civil engineering [34–36]. The advantages of the proposed models over the traditional models are:

(1) The random forest method is more suitable for establishing the complex nonlinear relationship between input and output parameters, because the difficulty of assuming the form of expression is avoided;

(2) A few samples from the original training set are randomly selected to form a sub-sample set, which allows each decision tree to be trained on a specific set of samples, thereby increasing the diversity of the model;

(3) For each node of decision tree, randomly selected features (i.e., input parameters), are considered when determining the best segmentation point. This can prevent some features from heavily influencing the predictive model, thus improving the robustness of the model;

(4) By averaging or weighted averaging the results of multiple decision trees, the final predicted value of the random forest model can be reliably obtained.

2.3. Realization of the Method

The step-by-step description of the methodology of the random forest machine learning method is illustrated as follows, and the schematic plot of the procedure to develop the *DMC* predictive models is as shown in Figure 1.

(1) Due to the lack of dynamic loading test data, a numerical model database was developed for training data. The numerical model needed to accurately simulate the dynamic mechanical behaviors of RC columns. Moreover, the critical design parameters of RC columns were considered and columns with the same parameters were designed to be under different strain rate levels.

(2) Based on the simulated results of mechanical behavior parameters, the dynamic modified coefficient (*DMC*) values in terms of the yielding bearing capacity, the ultimate bearing capacity and the ductility coefficient were obtained.

(3) Before the model was trained, the obtained data were divided into 80% for the training set (for training data) and 20% for the test set (for verification). Moreover, the parameters of the random forest algorithm were set, including the number of decision trees (N = 200) and the maximum depth of the forest (depth = 10), etc.

(4) When employing the random forest algorithm, the *DMC* values of the yielding bearing capacity, the ultimate bearing capacity and the ductility coefficient were treated as

outputs, and 5 structural parameters and the strain rate index introduced in Section 2.1 were selected as input variables.

(5) During the training process, the criterion of minimum mean square error (*MSE*) [29] was adopted for selecting features in construction of binary trees. The mean square error (i.e., *MSE*) was obtained by

$$MSE = \frac{1}{n}\sum_{i=1}^{n}(y_i - \hat{y})^2 \quad (5)$$

where n denotes the number of sample data, while y_i and $\hat{y}$ represent the value of sample data and the mean value. The *MSE* of randomly selected features and possible splitting point were calculated. The features and splitting point that minimized the weighted sum of the mean square error were selected for node splitting, and multiple decision trees were constructed.

(6) Finally, after the model was trained, by taking the average results of decision trees, the value of *DMC* predicted by the random forest model was acquired. The feature importance of the node was estimated to evaluate the contribution of each feature in influencing the results of the predictive models.

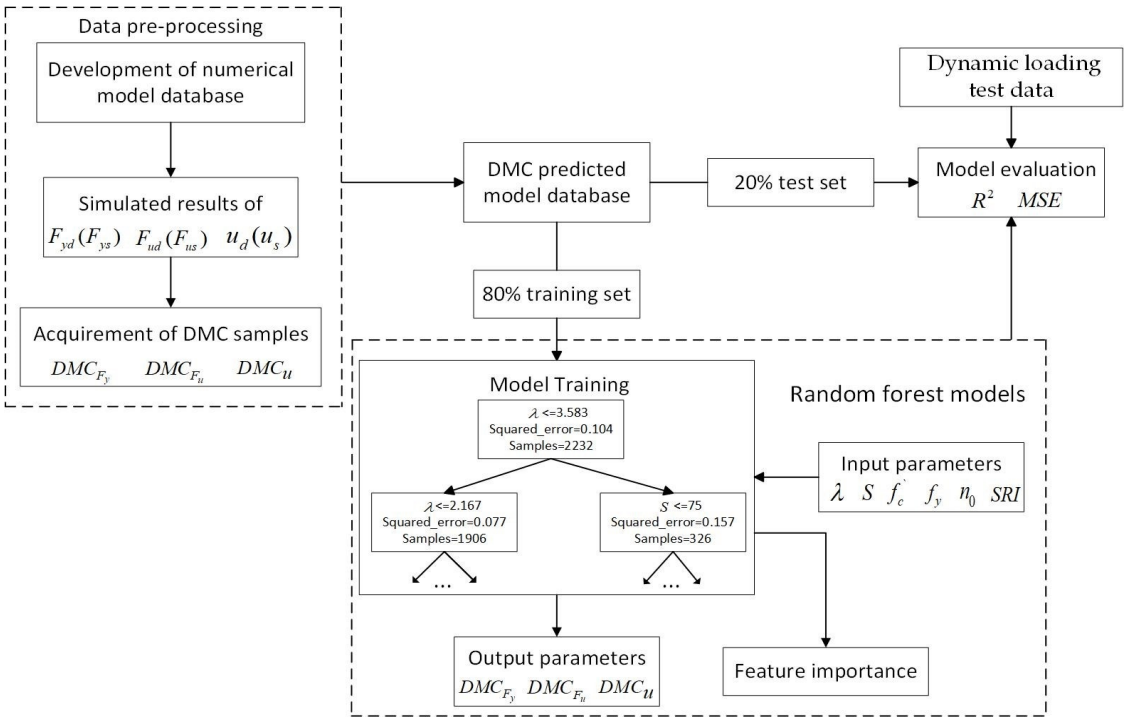

Figure 1. Illustration of procedure to develop the *DMC* predictive models.

3. Dynamic Modified Numerical Model of RC Columns

3.1. Establishment of Numerical Model

The developed numerical model of RC columns was composed of three sub-elements in series (see Figure 2), including the fiber beam-column element, the zero-length shear element and the bond-slip element to simulate the flexural deformation, the shear deformation and the bond-slip deformation, respectively. Based on the limit state material theory [37], the mechanical behaviors of column members under different failure modes could be simulated. Moreover, dynamic modifications were made to the three sub-elements to consider the influences of loading rate on the mechanical behavior and deformation mechanism of RC column members.

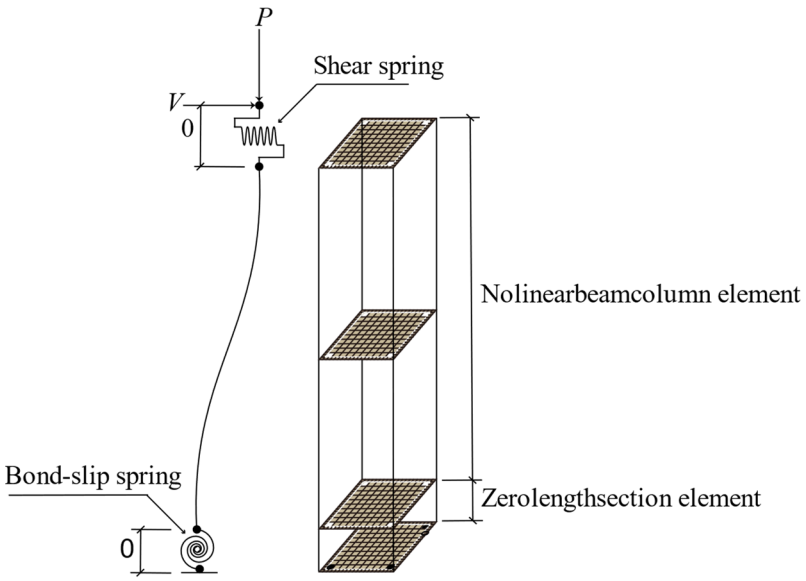

Figure 2. Illustration of the developed numerical model for RC columns.

The flexural sub-element was developed by using the force-based beam-column element on the OpenSees platform. The cross section of the flexural sub-element was divided by fibers and the uniaxial material constitutive models of reinforcing steel and concrete 04 were employed to depict the material properties of reinforcement and concrete, respectively. For reinforcement, the strength degradation under cyclic loading [38] and the buckling effect [39] were considered. As for concrete, the degradation of strength and stiffness during cyclic loading, and the enhancement of concrete strength and ductility [40] due to the constraint effect of stirrups were fully taken into account.

To consider the strain rate effect of materials on the flexural behavior of columns, the constitutive model parameters of reinforcement and concrete were dynamically modified by using the available empirical DIF equations [41,42]. The dynamic modified constitutive models and the static constitutive models of reinforcement and concrete are plotted in Figure 3. The parameters modified were the yielding strength f_y, the ultimate strength f_u and the initial hardening strain ε_h of reinforcement, and the compressive strength f_c', the tensile strength f_t, the elastic modulus E_c and the ultimate compressive strain ε_{cd} of concrete. The employed DIF equations are tabulated in Table 1.

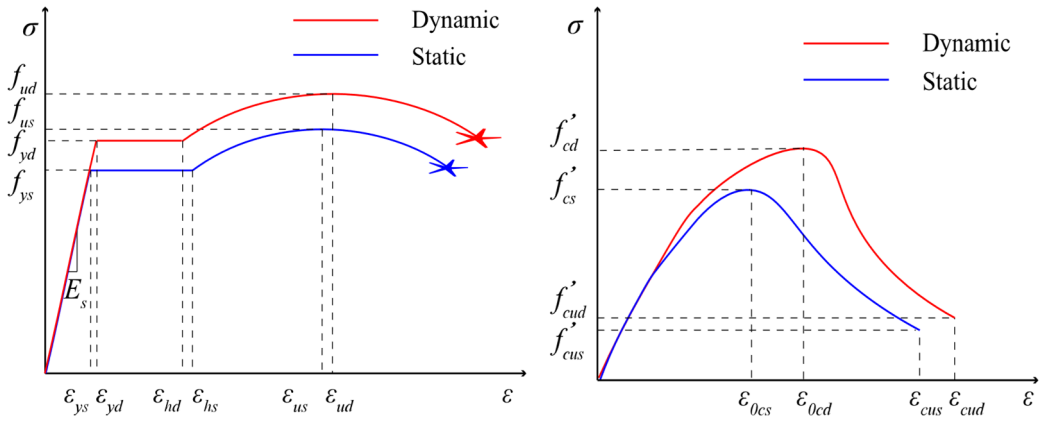

(**a**) Reinforcement (**b**) Concrete

Figure 3. Comparisons of static and dynamic constitutive models for RC materials. The star denotes the fracture failure point of reinforcement.

Table 1. DIF equations for dynamic modification to flexural sub-element.

Material	Parameter	Expression of DIF Model	Relevant Parameters
Concrete [42]	f'_c	$DIF_{f'_c} = \frac{f'_{cd}}{f'_{cs}} = \left(\frac{\dot{\varepsilon}_c}{\dot{\varepsilon}_{c0}}\right)^{1.026\alpha}, \dot{\varepsilon}_c \le 30/\mathrm{s}$ $DIF_{f'_c} = \frac{f'_{cd}}{f'_{cs}} = \gamma\left(\frac{\dot{\varepsilon}_c}{\dot{\varepsilon}_{c0}}\right)^{\frac{1}{3}}, \dot{\varepsilon}_c > 30/\mathrm{s}$	$\alpha = \frac{1}{5+\frac{f'_{cs}}{10}}$ $\log\gamma = 6.16\alpha - 2.0$
	f_t	$DIF_{f_t} = \frac{f_{td}}{f_{ts}} = \left(\frac{\dot{\varepsilon}_t}{\dot{\varepsilon}_{t0}}\right)^{1.016\alpha}, \dot{\varepsilon}_t \le 30s^{-1}$ $DIF_{f_t} = \frac{f_{td}}{f_{ts}} = \gamma\left(\frac{\dot{\varepsilon}_t}{\dot{\varepsilon}_{t0}}\right)^{\frac{1}{3}}, \dot{\varepsilon}_t > 30s^{-1}$	$\alpha = \frac{1}{10+6\frac{f'_{cs}}{10}}$ $\log\gamma = 7.11\alpha - 2.33$
	E_c	$DIF_{E_c} = \frac{E_{cd}}{E_{cs}} = \left(\frac{\dot{\varepsilon}_c}{\dot{\varepsilon}_{c0}}\right)^{0.026}$	-
	ε_{cd}	$DIF_{\varepsilon_c} = \frac{\varepsilon_{cd}}{\varepsilon_{cs}} = \left(\frac{\dot{\varepsilon}_c}{\dot{\varepsilon}_{c0}}\right)^{0.02}$	-
Reinforcement [43]	f_y	$DIF_{f_y} = \frac{f_{yd}}{f_{ys}} = 1 + c_f \lg\frac{\dot{\varepsilon}}{\dot{\varepsilon}_0}$	$c_f = 0.1709 - 3.289\times10^{-4} f_{ys}$
	f_u	$DIF_{f_u} = \frac{f_{ud}}{f_{us}} = 1 + c_u \lg\frac{\dot{\varepsilon}}{\dot{\varepsilon}_0}$	$c_u = 0.02783 - 2.982\times10^{-5} f_{ys}$
	ε_h	$DIF_{\varepsilon_h} = \frac{\varepsilon_{hd}}{\varepsilon_{hs}} = 1 + c_h \lg\frac{\dot{\varepsilon}}{\dot{\varepsilon}_0}$	$c_h = 0.9324 - 0.00212 f_{ys}$

Note: The subscripts 's' and 'd' denote the static and dynamic material parameters, respectively; $\dot{\varepsilon}_c$ and $\dot{\varepsilon}_{c0} = 3\times10^{-5}/\mathrm{s}$ represent the strain rates of compressive concrete under dynamic and static loading, respectively; $\dot{\varepsilon}_t$ and $\dot{\varepsilon}_{t0} = 3\times10^{-6}/\mathrm{s}$ represent the strain rates of tensile concrete under dynamic and static loading, respectively; $\dot{\varepsilon}$ and $\dot{\varepsilon}_0 = 2.5\times10^{-4}/\mathrm{s}$ denote the strain rates of reinforcement under dynamic and static loading, respectively.

In the numerical model, the shear stress–shear strain relationship obtained by the modified compression field theory (i.e., MCFT) [44] was used to derive the constitutive model of force-deformation for the shear sub-element. To consider the influence of dynamic effect on shear bearing capacity and shear deformation of RC columns, the following MCFT calculation equations were modified using the DIF equations of materials. The material parameters modified were the compressive strength f'_c, the tensile strength f_t and the elastic modulus E_c of concrete, and the yielding strength of longitudinal reinforcement and stirrups, i.e., f_y and f_{yt}. The MCFT equations considering the dynamic modification are listed in Table 2. The schematic plot of dynamic modified and the static constitutive models of shear force-deformation are compared in Figure 4.

Table 2. Dynamic modified MCFT equations for shear sub-element.

MCFT Equations [43]	Description	Modified Parameters
$f_2 \le \frac{f'_c \cdot DIF_{f_c}}{0.8-0.34\frac{\varepsilon_1}{\varepsilon_c}}\left[2\left(\frac{\varepsilon_2}{\varepsilon_c}\right) - \left(\frac{\varepsilon_2}{\varepsilon_c}\right)^2\right]$	The average compression stress f_2 should not exceed its allowable value.	f'_c
$f_1 = \varepsilon_1 \cdot E_c \cdot DIF_{E_c} \le \frac{f_t \cdot DIF_{f_t}}{1+\sqrt{500\varepsilon_1}}$	The average tensile stress f_1 should not exceed its allowable value.	f_t and E_c
$f_{yx} = E_s \cdot \varepsilon_{sx} \le f_y \cdot DIF_{f_y}$	The stress of longitudinal reinforcement should not exceed its dynamic yielding strength	f_y
$f_{yv} = E_s \cdot \varepsilon_{sv} \le f_{yt} \cdot DIF_{f_{yt}}$	The stress of stirrups should not exceed their dynamic yielding strength	f_{yt}
$v_{ci} \le v_{ci,\max} = \frac{\sqrt{f'_c \cdot DIF_{f'_c}}}{0.31+\frac{24w}{d_a+16}}$	The shear stress v_{ci} should not exceed the maximum allowable value $v_{ci,\max}$	f'_c

To accurately describe the dynamic behavior of the bond-slip sub-element, the constitutive model of bond stress-slip amount ($\tau - s$) in Equation (6) derived from the dynamic loading pull-out test results [44] was employed

$$F^{\tau}(s) = \begin{cases} \tau_u\left(2\sqrt{\frac{s}{s_0}} - \frac{s}{s_0}\right) & ,0 \le s \le s_0 \\ \tau_u\left(k_r + (1-k_r)\exp\left(\beta\left(\frac{s}{s_0}-1\right)^2\right)\right) & ,s > s_0 \end{cases} \quad (6)$$

where τ_u and s_0 represent the ultimate bond stress and the corresponding slip amount; β denotes the control coefficient for the descending branch of model; k_r is the ratio of residual bond stress to ultimate bond stress. The parameters τ_u, s_0 and β are relevant to the loading rate and the corresponding formulas are tabulated in Table 3.

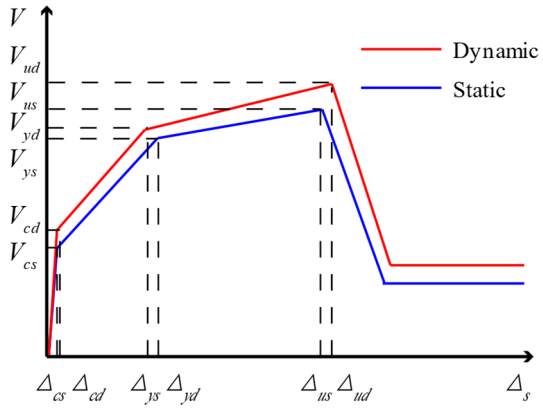

Figure 4. Comparisons of static and dynamic constitutive model of shear force-deformation.

Table 3. Parameters relevant to loading rate in the bond-slip model.

Parameter	Formulas
Ultimate bond stress τ_u	$\frac{\tau_u}{\sqrt{f'_{cu}}} = a + b\lg\frac{\dot{v}}{\dot{v}_0}$
Slip amount s_0	$s_0 = g + f\lg\frac{\dot{v}}{\dot{v}_0}$
Control coefficient β	$\beta = m + n\lg\frac{\dot{v}}{\dot{v}_0}$

Note: $\dot{v}$ and $\dot{v}_0 = 0.01$mm/s denote the dynamic and static loading rates, respectively; a, b, g, f, m and n are regression coefficients determined from the dynamic loading experiments [44].

Figure 5 illustrates the comparison results of static and dynamic bond-slip constitutive models. It can be observed that with the increase of loading rate, the ultimate bond stress τ_u is magnified and the slip amount s_0 is reduced, while the model shape is slightly changed.

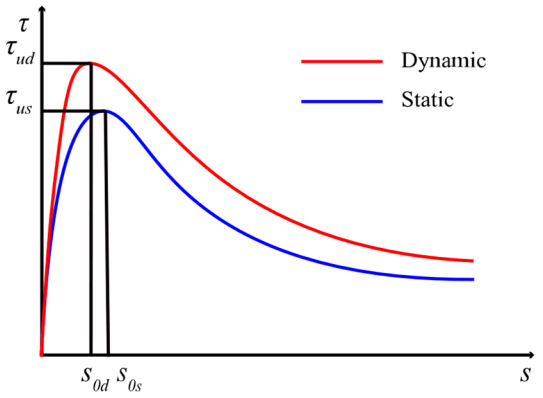

Figure 5. Comparisons of static and dynamic bond-slip constitutive models.

The bond-slip material [45] defining the relationship between longitudinal reinforcement stress and pull-out amount ($\sigma_s - S$) was employed to simulate the end rotation of columns caused by the bond-slip effect [46,47]. To acquire the pull-out amount S at column end at the given yielding strength f_y and ultimate strength f_u of longitudinal reinforcement, the micro-element method elaborated in [48] was adopted. The calculation process was realized through a self-compiled program using the Python language. Concrete 01 and the modified hysteric constitutive model were used for concrete and reinforcement in the

bond-slip sub-element, respectively. The dynamic modified and the corresponding static constitutive models are plotted in Figure 6. Based on the DIF equations [42], the constitutive model parameters of reinforcement in the zero-length bond-slip spring were modified. The modified parameters included the yielding strength f_y, the strain at yielding strength ε_y, the ultimate strength f_u and the slope of the hardening branch E_h. The corresponding formulas are presented in Table 4.

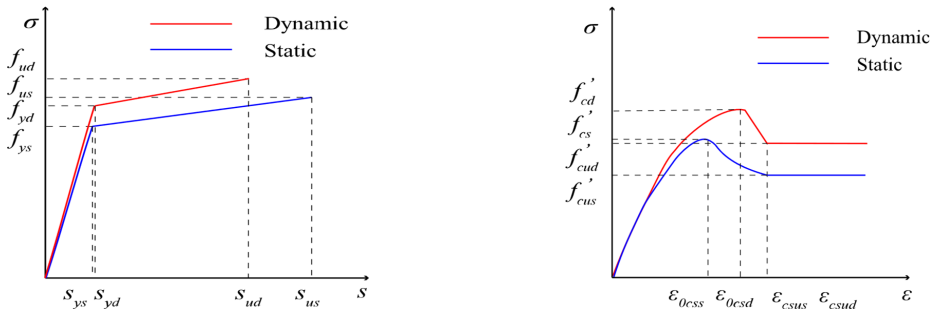

(**a**) Reinforcement (**b**) Concrete

Figure 6. Comparisons of static and dynamic constitutive models in bond-slip sub-elements.

Table 4. Dynamic modified parameters for bond-slip sub-element [42].

Parameter	Expression of Dynamic Modification
Yielding strength f_y,	$f_{yd} = f_y \cdot DIF_{f_y}$
Strain at yielding strength ε_y	$f_{ud} = f_u \cdot DIF_{f_u}$
Ultimate strength f_u	$\varepsilon_{yd} = \frac{f_{yd}}{f_{ys}}\varepsilon_y = DIF_{f_y} \cdot \varepsilon_y$
Slope of hardening branch E_h	$E_{hd} = \frac{f_u \cdot DIF_{f_u} - f_y \cdot DIF_{f_y}}{\varepsilon_u - DIF_{f_y} \cdot \varepsilon_y}$

3.2. Influences of Model Complexity on the Simulated Results

To investigate the influences of dynamic modification to sub-elements on the numerical results, six models with different complexities were established, as shown in Figure 7. By analyzing the results of Model-1/Model-2 (single sub-element), Model-3/Model-4 (two sub-elements) and Model-5/Model-6 (three sub-elements), the difference in simulated hysteretic curves using numerical models with different sub-elements was investigated. By comparing the simulated results of Model-1/Model-3/Model-5 (without dynamic modification) and Model-2/Model-4/Model-6 (with dynamic modification), the impact of dynamic modification on the hysteretic behaviors of RC columns was revealed.

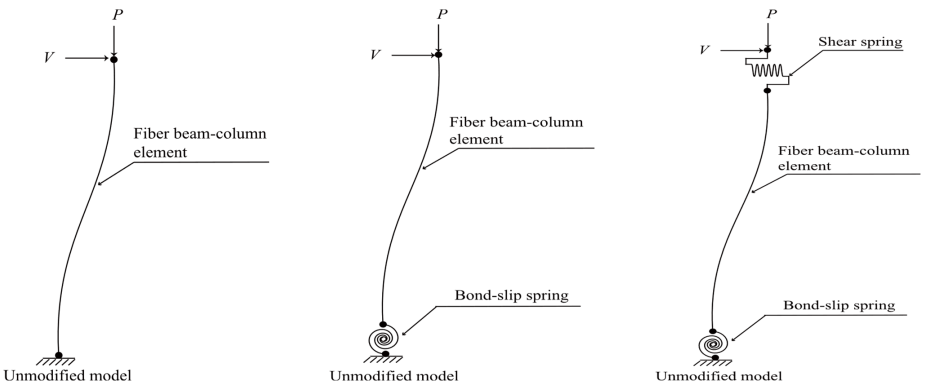

(**a**) Model-1 (**b**) Model-3 (**c**) Model-5

Figure 7. *Cont.*

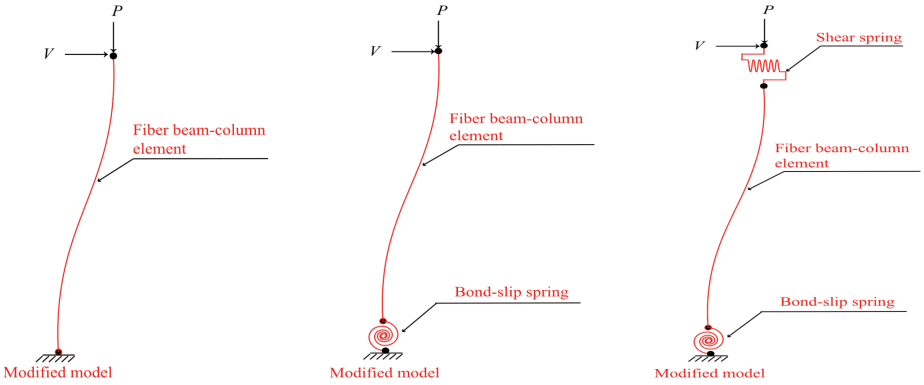

(**d**) Model-2 (**e**) Model-4 (**f**) Model-6

Figure 7. Numerical models with different complexities.

Figures 8–10 show the influences of the modeling approach on simulated hysteric behavior of three represented RC columns. Case-1, Case-2 and Case-3 were predicted to be under flexural, shear-flexural and shear failure modes, respectively. The design parameters of RC columns for case study are listed in Table 5. The critical mechanical behavior points, i.e., the yielding point, the ultimate point and the failure point, are also marked in the figures. The ductility coefficient is defined as the ratio of ultimate displacement to the yielding displacement. The yielding point was obtained by using the average results of the energy equivalent method, the geometric method and the R-PARK method. The failure point was taken as the point when the bearing capacity dropped to 85% of the ultimate bearing capacity.

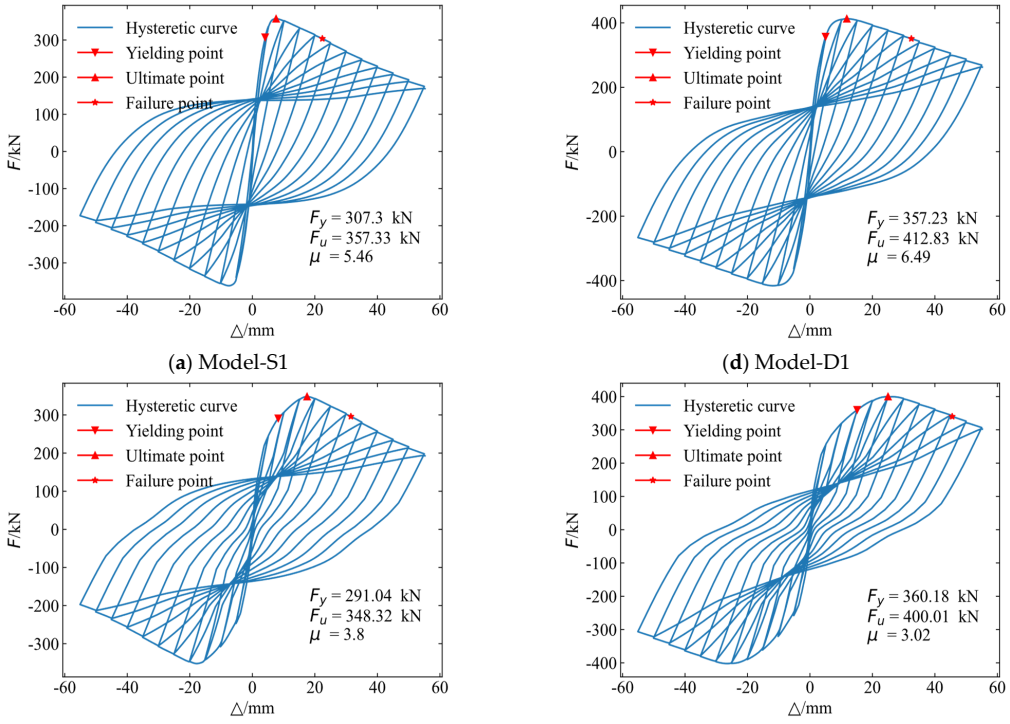

(**a**) Model-S1 (**d**) Model-D1

(**b**) Model-S2 (**e**) Model-D2

Figure 8. *Cont.*

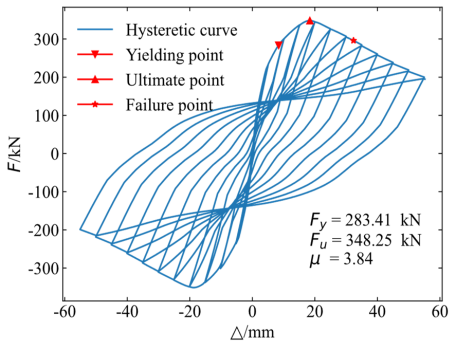

(**c**) Model-S3

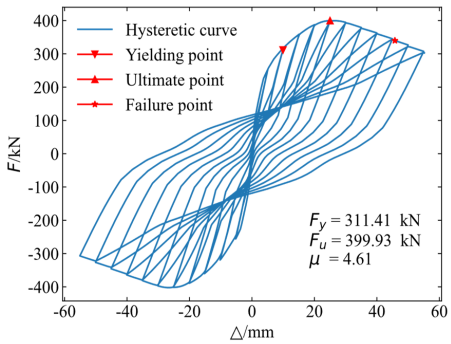

(**f**) Model-D3

Figure 8. Comparisons between hysteretic curves using different numerical models for Case-1.

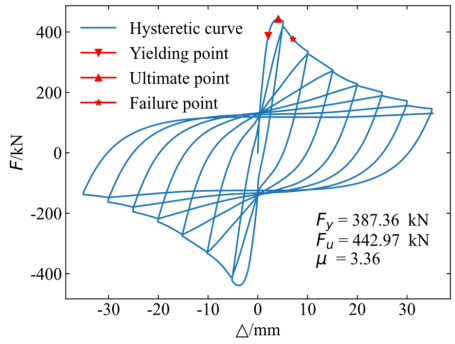

(**a**) Model-S1

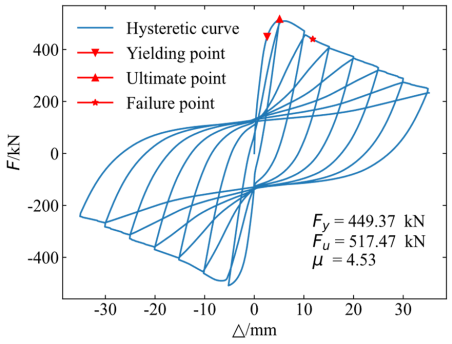

(**d**) Model-D1

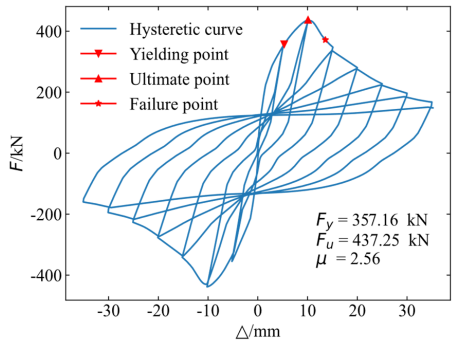

(**b**) Model-S2

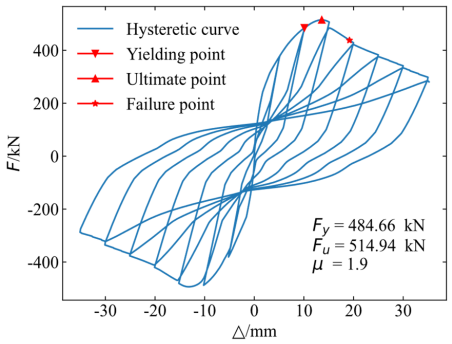

(**e**) Model-D2

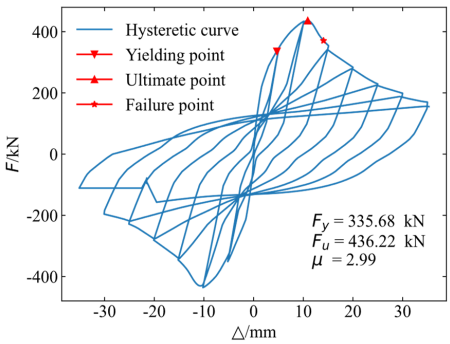

(**c**) Model-S3

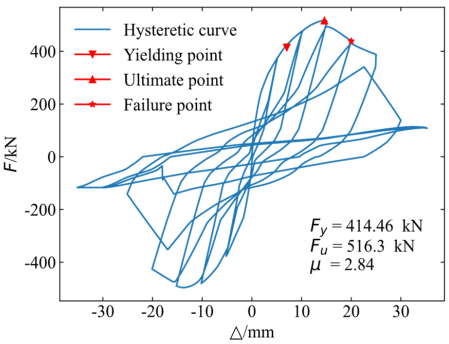

(**f**) Model-D3

Figure 9. Comparisons between hysteretic curves using different numerical models for Case-2.

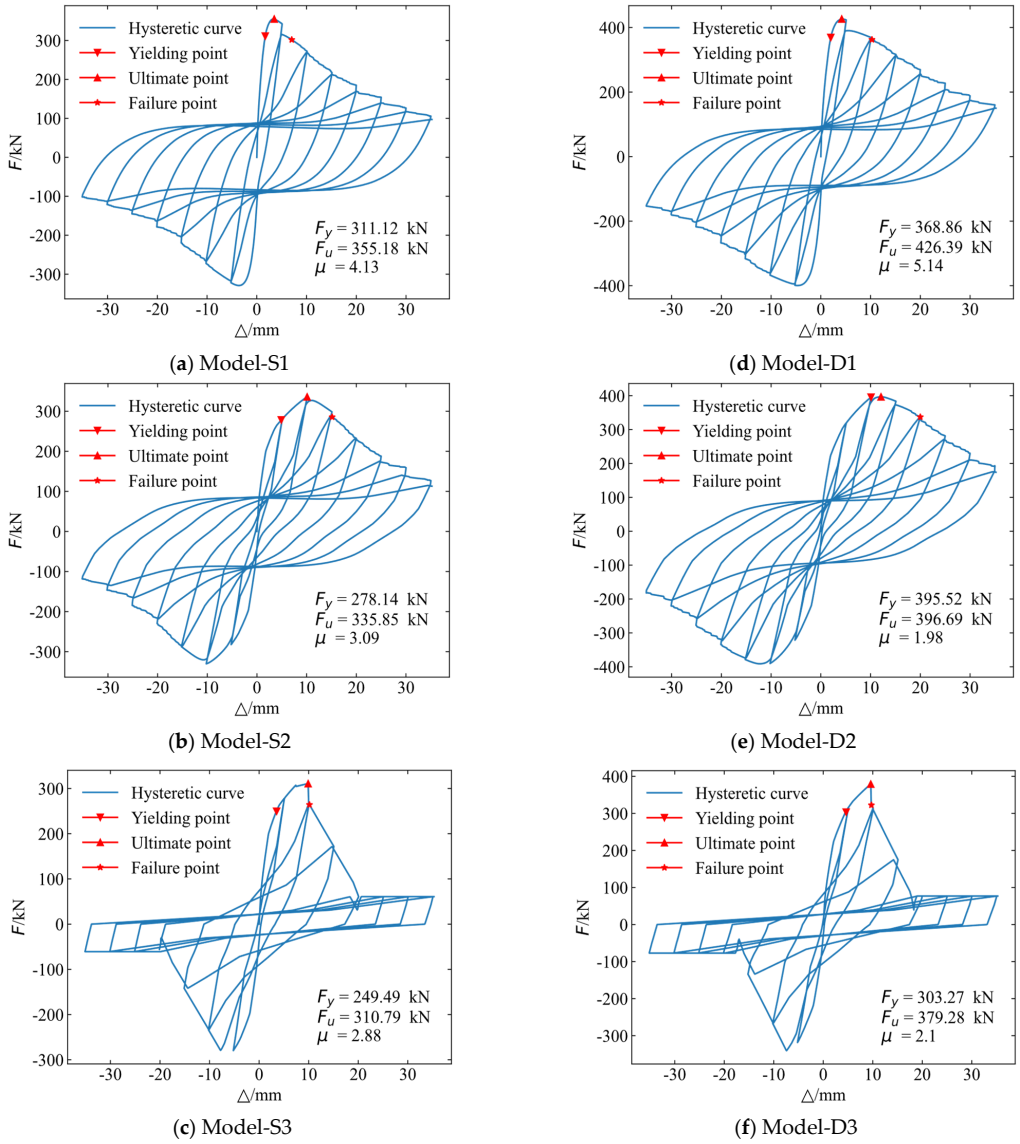

Figure 10. Comparisons between hysteretic curves using different numerical models for Case-3.

Table 5. Design parameters of RC columns for case study.

No.	Geometric Size (mm)	f_c' (MPa)	f_y (MPa)	λ	ρ_l (%)	S (mm)	n_0	Failure Mode
Case-1	300 × 300 × 800	50	500	2.67	2.26%	50	0.4	Flexural
Case-2	300 × 300 × 550	50	400	1.83	2.26%	50	0.2	Flexural-shear
Case-3	300 × 300 × 550	30	335	1.83	2.26%	50	0.4	Shear

Note: λ = shear span ratio of RC column members; ρ_l = longitudinal reinforcement ratio; S = stirrup spacing and n_0 = axial load ratio.

For Case-1, by comparing the group of static models shown in Figure 8a–c, it was found that the inclusion of bond-slip sub-element had a considerable impact on the simulated result of ductility while the influence of the shear sub-element was minor. By comparing the group of dynamic models shown in Figure 8d–f, it can be observed that the influences of sub-elements were more significant when considering the dynamic effect. For Case-2 and Case-3, by comparing Figure 9a–c (or Figure 10a–c), it was found that the inclusion of the shear sub-element had a considerable impact on the simulated result of hysteretic behavior as compared with the bond-slip sub-element. As the bond-slip sub-element was considered (Figures 9e and 10e), the enhancement of bearing capacity induced by dynamic

modification was more obvious for columns under flexural-shear and shear failure modes; when the shear sub-element was further incorporated for columns under flexural-shear failure mode (Figure 9f), the hysteretic curve exhibited accelerated degradation in the failure stage. For columns under shear failure mode, the degradation of bearing capacity and stiffness in Model-6 (Figure 10f) was comparatively more significant.

Furthermore, the results of bearing capacity and displacement ductility between the numerical models with and without the dynamic modification are quantitatively compared in Table 6. For the three representative cases, it was found that the dynamic modification to a single sub-element led to an increase of bearing capacity and an increase of ductility, while the dynamic modification to two and three sub-elements led to an increase of bearing capacity and a decrease of ductility. Due to the fact that in most dynamic loading test results the ductility of RC columns exhibited a decreasing trend [6,7], it was more reliable to simulate the hysteretic behavior of RC columns with bond-slip and shear sub-elements. Moreover, to more accurately simulate the mechanical behaviors of RC columns under seismic loading rate, dynamic modification also needed to be taken into account.

Table 6. Comparison results between the numerical models.

NO.	Model-D1/-S1		Model-D2/-S2		Model-D3/-S3	
	$\frac{F_{ud}-F_{us}}{F_{us}}$	$\frac{\mu_d-\mu_s}{\mu_s}$	$\frac{F_{ud}-F_{us}}{F_{us}}$	$\frac{\mu_d-\mu_s}{\mu_s}$	$\frac{F_{ud}-F_{us}}{F_{us}}$	$\frac{\mu_d-\mu_s}{\mu_s}$
Case 1	15.53%	18.89%	15.84%	−20.58%	14.83%	−5.19%
Case 2	16.01%	34.89%	35.69%	−25.91%	32.91%	−22.67%
Case 3	20.04%	24.34%	18.81%	−35.92%	22.04%	−26.36%

3.3. Validation of Numerical Model

To verify the accuracy of the proposed numerical model, the simulated backbone curves of RC columns obtained by the dynamic modified model and unmodified model were compared with the measured results from different experiments [4,7,10], as presented in Figure 11. The critical mechanical behavior points, i.e., the yielding point, the ultimate point and the failure point are also plotted in the figures. It was observed that the backbone curves from the elastic stage to the descending stage of RC columns could be well estimated by employing the dynamic modified numerical model. As compared with the commonly used unmodified model, the dynamic modified model provided more accurate predicted results for the backbone curve of RC columns under a dynamic loading rate.

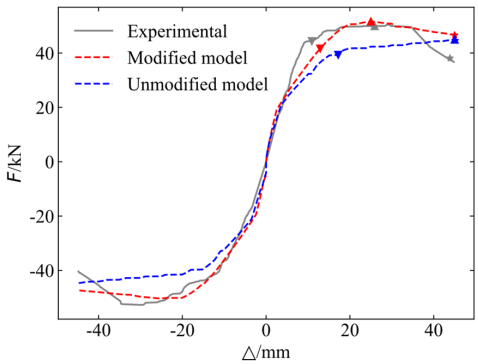

(**a**) D2

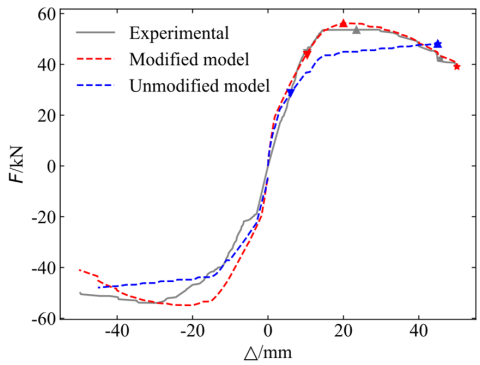

(**d**) D7

Figure 11. *Cont.*

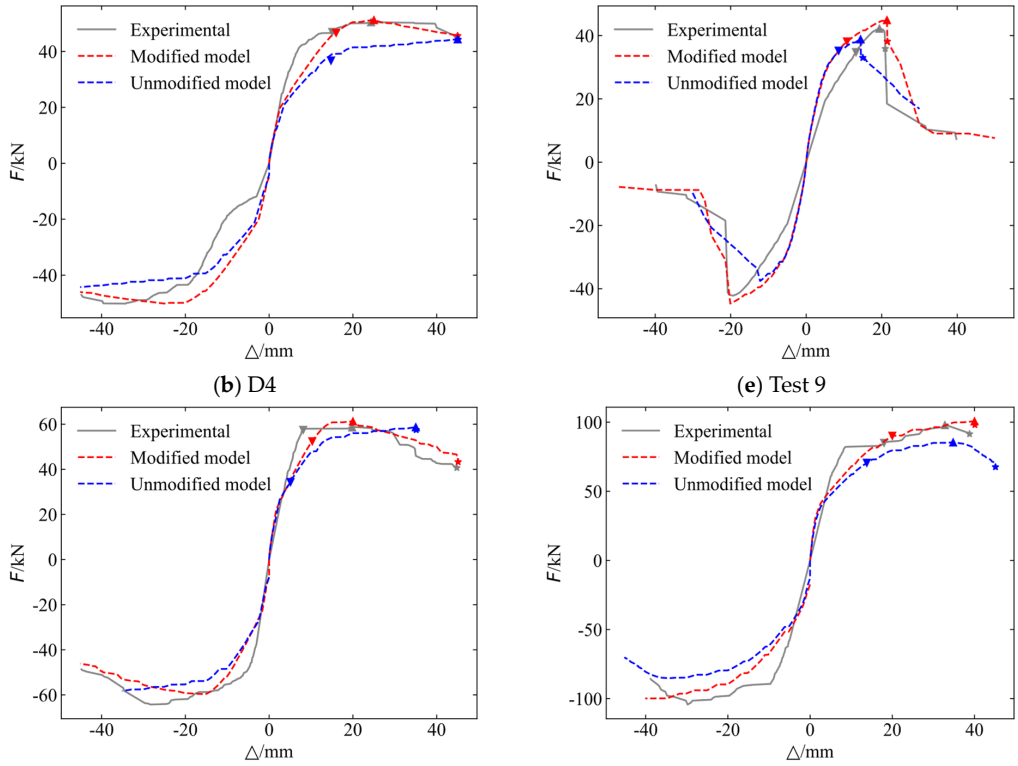

Figure 11. Validation results of backbone curve in modified and unmodified numerical models.

4. Development of Numerical Model Database

Given the lack of dynamic loading test results, the training data for the random forest algorithm were based on the results of the proposed numerical model. For this paper, a total of 930 × 4 = 3720 numerical models were established to develop the numerical model database. Four levels of strain rate (10^{-5}/s, 10^{-3}/s, 10^{-2}/s, 10^{-1}/s) were taken into account. Under each strain rate level, 930 numerical models of columns were established considering different structural parameters, such as the concrete compressive strength (30–50 MPa), the reinforcement yielding strength (335–500 MPa), the shear span ratio (1.67–3.83), the axil load ratio (0.2–0.6) and the stirrup spacing (50–50 mm). It is noted that the above structural parameters were uniformly distributed on the corresponding interval and randomly assigned to form the basic structural design parameters for a numerical model of the columns. Although the numerical models were designed for the Chinese building design code specifically, the proposed method and research conclusions can be extended to foreign situations and other materials.

Based on the numerical results, the bearing capacity and displacement at yielding point, the ultimate point and the failure point were determined using the same approach illustrated in Section 3.2. In the database, the numerical samples obtained under strain rate levels (10^{-3}/s, 10^{-2}/s, 10^{-1}/s) were treated as the dynamic mechanical behavior parameters, whereas the numerical samples under strain rate level of 10^{-5}/s were considered as the corresponding static mechanical behavior parameters. Then, the values of DMC_{F_y},DMC_{F_u} and DMC_{μ} were calculated by employing Equations (1)–(3). The predictive models of *DMC* were developed by 80% of the *DMC* values. In that case, the total number of training data were 930 × 3 × 80% = 2232.

5. Predicted Results Using the Model

5.1. Results of Feature Importance

To evaluate the feature importance of each node, the weighted reduction in *MSE* (i.e., the sum of reduction in *MSE* before and after splitting of features multiplied by the

proportion of sample number on each leaf node) was calculated. To compare the relative importance of each feature, the results of feature importance for all nodes were further normalized. The results of feature importance are presented in Figure 12. The detailed values of feature importance and the ranking order are given in Table 7.

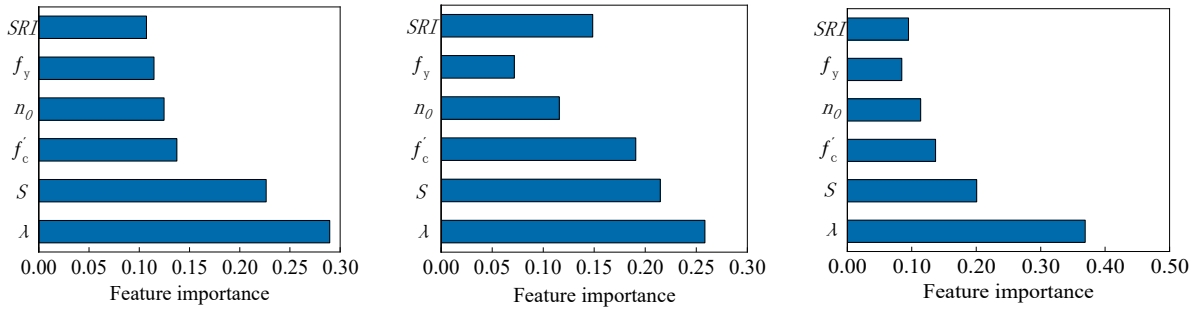

(**a**) DMC_{F_y} (**b**) DMC_{F_u} (**c**) DMC_{μ}

Figure 12. Feature importance of the developed *DMC* models.

Table 7. Results of feature importance and ranking.

***DMC* Model**	**Ranking of Feature Importance**					
	1	**2**	**3**	**4**	**5**	**6**
DMC_{F_y}	λ 0.2896	S 0.2264	f_c' 0.1374	n_0 0.1247	f_y 0.1147	SRI 0.1071
DMC_{F_m}	λ 0.2585	S 0.2147	f_c' 0.1908	SRI 0.1485	n_0 0.1158	f_y 0.0717
DMC_{μ}	λ 0.3691	S 0.2008	f_c' 0.1369	n_0 0.1137	SRI 0.0950	f_y 0.0845

It can be concluded that the shear span ratio λ was the most important feature parameter that affected the three predictive models of *DMC*, following by the stirrup spacing S and the concrete strength f_c'. For the three *DMC* models, differences were found as to the order of the 4th to 6th important features. Feature importance could be used to measure the contribution of each feature in influencing the results of the predictive models, which optimized the process of feature selection during model training [49]. It should be mentioned that for the random forest method, random seeds or model parameters may lead to different results of feature selection, indicating that the importance of features is dependent on the training set, including the distribution of data, the sample size and the randomness of the model.

5.2. Validation of DMC Models

Figure 13 shows the validation results of *DMC* models in terms of the yielding bearing capacity, the ultimate bearing capacity and the ductility coefficient, respectively. The prediction points marked by the red triangle and the y = x line denoted by the dash line are plotted in the figure. If the predicted value was exactly the same as the actual value, the point is on the y = x line. In other words, the closer the point was to the y = x line, the more accurate was the predicted result. From the distribution of the scatter plots, it can be observed that the predicted points are distributed around the y = x line, indicating that the developed *DMC* models were capable of predicting the influences of dynamic effect on the mechanical behavior parameters, i.e., the yielding bearing capacity, the ultimate bearing capacity and the ductility coefficient of RC columns.

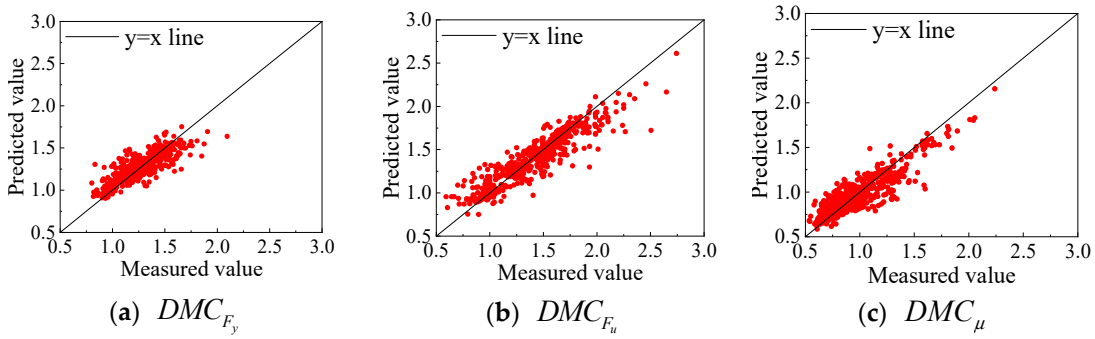

Figure 13. Validation results of the developed *DMC* models.

To further verify the model accuracy, the developed models were employed to predict the *DMC* values in terms of the yielding capacity, the ultimate capacity and the ductility coefficient (i.e., DMC_{F_y}, DMC_{F_u} and DMC_{μ}) of RC columns at three levels of strain rate, i.e., 10^{-3}/s, 10^{-2}/s and 10^{-1}/s, respectively, as shown in Figure 14. It was found that the predictive models provided good estimated results of the *DMC* values at different strain rate levels.

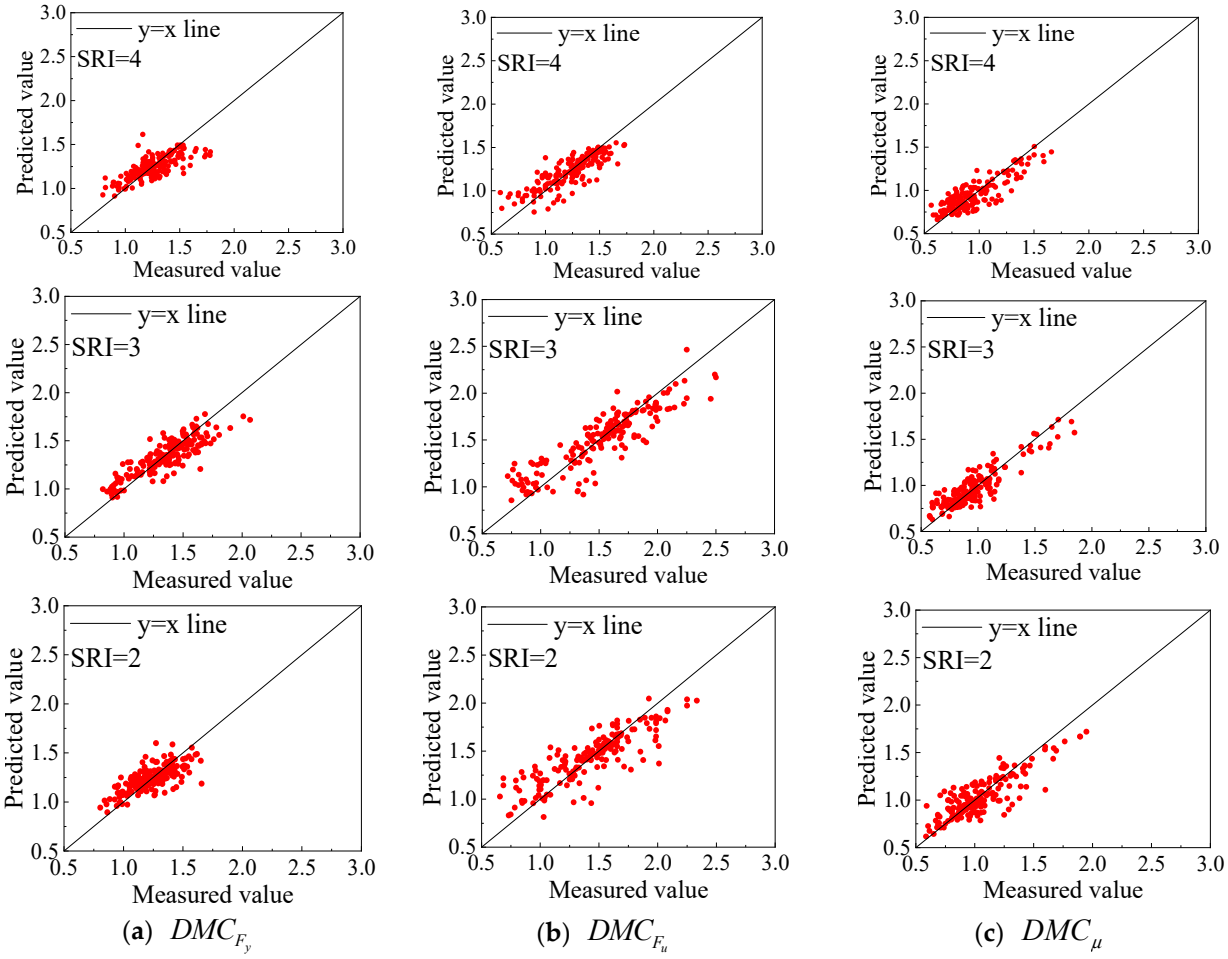

Figure 14. Validation results of *DMC* models at different strain rate levels.

Moreover, the effectiveness of the developed models was verified by the test results of 13 RC column specimens from available dynamic loading experiments [9]. Figure 15 shows the comparison results of measured and predicted *DMC* values. It is noted that the test strain rate of the longitudinal reinforcement was used to obtain the strain rate index. The

R-square and the mean square error were 0.72 and 0.003 for the predictive model of DMC_{F_y}, 0.76 and 0.001 for the predictive model of DMC_{F_u}, 0.68 and 0.001 for the predictive model of DMC_{μ}, respectively. By taking the structural design parameters and the calculated *SRI* of each column specimen as inputs, it was found that the predictive models developed by the random forest method provided accurate results estimating the change in yielding and ultimate bearing capacity and ductility coefficient of column members under different seismic loading rates.

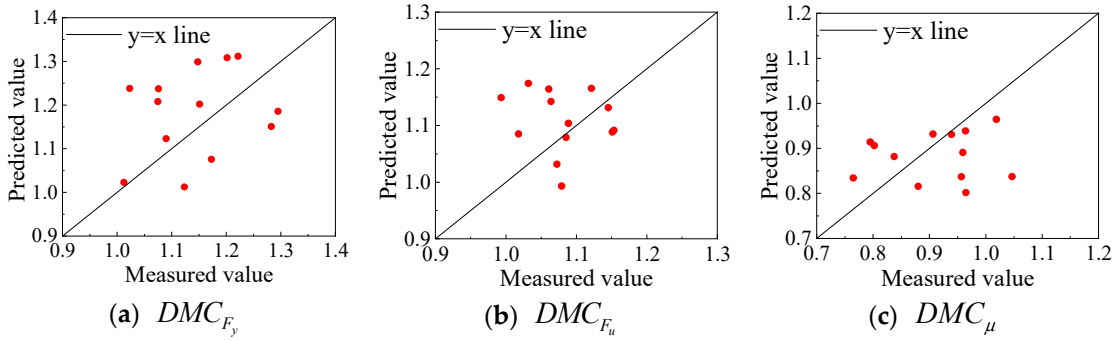

Figure 15. Validation results of *DMC* models using available dynamic loading test data.

5.3. Evaluation of Model Precision

To evaluate the goodness of fit for the developed *DMC* models, the R-square (R^2) and the mean square error (*MSE*) were used in this paper, which are defined as follows

$$R^2 = 1 - \frac{SS_{res}}{SS_{tot}} \tag{7}$$

where SS_{res} denotes the sum of squares for residuals, and SS_{tot} denotes the sum of squares for total.

$$MSE = \frac{1}{n}\sum_{i=1}^{n}(Y_i - \hat{Y}_i)^2 \tag{8}$$

where Y_i denotes the predicted value, $\hat{Y}_i$ denotes the actual value, respectively.

The fitting precision of the *DMC* models as to the total of the testing set and the three sub-testing sets at different levels of strain rate is tabulated in Table 8.

Table 8. Evaluation results of *DMC* model precision.

Model	*SRI* (Total)		*SRI* = 4		*SRI* = 3		*SRI* = 2	
	R^2	*MSE*	R^2	*MSE*	R^2	*MSE*	R^2	*MSE*
DMC_{F_y}	0.67	0.01	0.61	0.01	0.70	0.02	0.61	0.01
DMC_{F_u}	0.77	0.03	0.69	0.02	0.82	0.03	0.77	0.03
μ	0.70	0.02	0.61	0.02	0.75	0.02	0.68	0.03

It was found that the models provided accurate and reliable predictive results with the test data. Moreover, it should be mentioned that due to the fact that different failure modes of RC columns were not distinguished in the development of *DMC* models (i.e., all the data were mixed), this may have exerted a certain impact on the precision of the predictive models. Thus, further studies are needed to improve the applicability of the models.

6. Conclusions

In this paper, for accurately estimating the dynamic mechanical behaviors of RC column members, predictive models of the dynamic modified coefficient (*DMC*) were developed based on the random forest method and a numerical model database. The main conclusions are summarized as follows:

(1) By training a large number of data using the random forest method, the *DMC* predictive models of yielding capacity, ultimate capacity and ductility coefficient for RC columns were developed. Accuracy of the proposed models has been verified using the reserved 20% data and experimental data. Given the structural design parameters as inputs, the proposed models can be used to rapidly evaluate the dynamic mechanical behaviors of RC columns under seismic loading rates.

(2) The numerical model of RC columns was established by dynamic modification to different deformation sub-elements. It can provide accurate and effective simulated results of the dynamic mechanical behaviors of RC columns, making up for the deficiency of insufficient test data. By comparing the simulated hysteretic curves using numerical models with different complexities, the necessity of incorporating shear and bond-slip sub-elements and dynamic modification was revealed.

(3) By analyzing the feature importance, it was found that the shear span ratio was the most important factor affecting the *DMC* models, followed by the stirrup spacing and the concrete compressive strength. For the three *DMC* models, differences were found as to the order of the 4th to 6th important features. The results of feature importance were dependent on the training data; however, it provided a reference to measure the contribution of input parameters to the results of the developed predictive models.

(4) In future research works, the accuracy of predictive models can be improved by distinguishing different failure modes of RC columns and the machine learning method can be improved to develop explainable predictive models. For dynamic analysis of structural systems considering the change in strain rate, a program of real-time dynamic modification to constitutive models of deformation sub-elements needs to be developed. Moreover, the proposed numerical model and method can be applied to other types of structural members.

Author Contributions: Conceptualization, R.-H.L.; methodology, R.-H.L., M.-Y.L. and X.-Y.Z.; software and validation, M.-Y.L. and X.-Y.Z.; resources and writing—original draft preparation, R.-H.L. and X.-W.Z.; review and editing, R.-H.L.; visualization, M.-Y.L. and X.-Y.Z. All authors have read and agreed to the published version of the manuscript.

Funding: This research was funded by the National Natural Science Foundation of China, grant number No. 52108438) and the Open Fund of National Center for International Research of Subsea Engineering Technology and Equipment grant number No. 3132023362.

Data Availability Statement: The data supporting the conclusions of this article will be made available by the authors on request.

Acknowledgments: The authors express great thanks to Yuan Zhang (an engineer from the Northeast Branch of China Construction Eighth Engineering Bureau Division Corp. Ltd.) for providing valuable technical support in completing this research work.

Conflicts of Interest: The authors declare no conflict of interest.

References

1. Fu, H.C.; Erki, M.A.; Seckin, M. Review of effects of loading rate on reinforced concrete. *J. Struct. Eng.* **1991**, *117*, 3660–3679. [CrossRef]
2. Chen, H.B.; Su, Y.P.; Xing, J.W.; Zhang, Y.M. Experimental research on constitute relation of concrete under uniaxial tension and compression with different strain rate. *Adv. Mater. Res.* **2011**, *250–253*, 3279–3283. [CrossRef]
3. Feng, L.; Yu, D.; Kuang, X.; Le, L. Strain Rate Behavior in Tension of Reinforcing Steels HPB235, HRB335, HRB400, and HRB500. *Materials* **2016**, *9*, 1013.
4. Ghannoum, W.; Saouma, V.; Haussmann, G.; Polkinghorne, K.; Eck, M.; Kang, D.H. Experimental investigations of loading rate effects in reinforced concrete columns. *J. Struct. Eng.* **2012**, *138*, 1032–1041. [CrossRef]
5. Jiang, Z. *Dynamic Loading Experiment and Numerical Simulation Study on Reinforced Concrete Columns*; Hunan University: Changsha, China, 2012. (In Chinese)
6. Otani, S.; Kaneko, T.; Shiohara, H. *Strain Rate Effect on Performance of Reinforced Concrete Members*; Kajima Technical Research Institute, Kajima Corporation: Tokyo, Japan, 2003.

7. Wang, D.B.; Li, H.N.; Li, G. Experimental study on dynamic mechanical properties of reinforced concrete column. *J Reinf. Plast. Comp.* **2013**, *32*, 1793–1806. [CrossRef]
8. Li, H.N.; Li, R.H.; Li, C.; Wang, D.B. Development of hysteretic model with dynamic effect and deterioration for seismic-performance analysis of reinforced concrete structures. *J. Struct. Eng.* **2020**, *146*, 04020215. [CrossRef]
9. Wang, D.B.; Li, H.N.; Li, G. Experimental tests on reinforced concrete columns under multi-dimensional dynamic loadings. *Constr. Build. Mater.* **2013**, *47*, 1167–1181. [CrossRef]
10. Jiang, Z.; Xu, B.; Zeng, X.; Tang, L. Dynamic load-displacement behavior simulation of RC columns considering strain rate and nonlinearity effects. *Adv. Mater. Res.* **2010**, *163–167*, 1811–1818. [CrossRef]
11. Valipour, H.R.; Luan, H.; Foster, S.J. Analysis of RC beams subjected to shock loading using a modified fibre element formulation. *Comput. Concr.* **2009**, *6*, 377–390. [CrossRef]
12. Ožbolt, J.; Sharma, A. Numerical simulation of reinforced concrete beams with different shear reinforcements under dynamic impact loads. *Int. J. Impact Eng.* **2011**, *38*, 940–950. [CrossRef]
13. Xiao, S.Y. Numerical study of dynamic behaviour of RC beams under cyclic loading with different loading rates. *Mag. Concr. Res.* **2015**, *67*, 325–334. [CrossRef]
14. Rouchette, A.; Zhang, W.P.; Chen, H. Simulation of Flexural Behavior of Reinforced Concrete Beams under Impact Loading. *Appl. Mech. Mater.* **2013**, *351–352*, 1018–1023. [CrossRef]
15. Adhikary, S.D.; Li, B.; Fujikake, K. Dynamic behavior of reinforced concrete beams under varying rates of concentrated loading. *Int. J. Impact Eng.* **2012**, *47*, 24–38. [CrossRef]
16. Song, Y.; Wang, J.; Han, Q. Dynamic performance of flexure-failure-type rectangular RC columns under low-velocity lateral impact. *Int. J. Impact Eng.* **2023**, *175*, 104541. [CrossRef]
17. Adhikary, S.D.; Li, B.; Fujikake, K. Strength and behavior in shear of reinforced concrete deep beams under dynamic loading conditions. *Nucl. Eng. Des.* **2013**, *259*, 14–28. [CrossRef]
18. Li, R.H.; Li, H.N.; Li, C. Dynamic modified model for RC columns based on experimental observations and Bayesian updating method. *J. Eng. Mech.* **2019**, *145*, 04019005. [CrossRef]
19. Rayjada, S.P.; Raghunandan, M.; Ghosh, J. Machine learning-based RC beam-column model parameter estimation and uncertainty quantification for seismic fragility assessment. *Eng. Struct.* **2023**, *278*, 115111. [CrossRef]
20. Abdellatif, S.; Raza, A. Machine learning model for predicting ultimate capacity of FRP-reinforced normal strength concrete structural elements. *Struct. Eng. Mech.* **2023**, *85*, 315–335. [CrossRef]
21. Mai, H.-V.T.; Nguyen, M.H.; Trinh, S.H.; Ly, H.-B. Optimization of machine learning models for predicting the compressive strength of fiber-reinforced self-compacting concrete. *Front. Struct. Civ. Eng.* **2023**, *17*, 284–305. [CrossRef]
22. Li, J.; Pang, Y.; Mu, Q.; Zhang, X.; Shi, Y.; Wang, H. Post-blast capacity evaluation of concrete-filled steel tubular (CFST) column based on machine learning technique. *Adv. Struct. Eng.* **2023**, *26*, 11. [CrossRef]
23. Megalooikonomou, K.G.; Beligiannis, G.N. Random Forests Machine Learning Applied to PEER Structural Performance Experimental Columns Database. *Appl. Sci.* **2023**, *13*, 12821. [CrossRef]
24. Kim, S.; Hwang, H.; Oh, K.; Shin, J. A Machine-Learning-Based Failure Mode Classification Model for Reinforced Concrete Columns Using Simple Structural Information. *Appl. Sci.* **2024**, *14*, 1243. [CrossRef]
25. Huang, C.; Li, Y.; Gu, Q.; Liu, J. Machine learning–based hysteretic lateral force-displacement models of reinforced concrete columns. *J. Struct. Eng.* **2022**, *148*, 04021291. [CrossRef]
26. Liu, Z.; Guo, A. Empirical-based support vector machine method for seismic assessment and simulation of reinforced concrete columns using historical cyclic tests. *Eng. Struct.* **2021**, *237*, 112141. [CrossRef]
27. Todorov, B.; Billah, A.H.M.M. Machine learning driven seismic performance limit state identification for performance-based seismic design of bridge piers. *Eng. Struct.* **2022**, *255*, 113919. [CrossRef]
28. Luo, H.; Paal, S.G. Machine Learning-Based Backbone Curve Model of Reinforced Concrete Columns Subjected to Cyclic Loading Reversals. *J. Comput. Civ. Eng.* **2018**, *32*, 04018042. [CrossRef]
29. Feng, D.C.; Liu, Z.T.; Wang, X.D.; Jiang, Z.; Liang, S.X. Failure mode classification and bearing capacity estimation for reinforced concrete columns based on ensemble machine learning algorithm. *Adv. Eng. Inform.* **2020**, *45*, 101126. [CrossRef]
30. Malvar, L.J.; Crawford, J.E. Review of static and dynamic properties of steel reinforcing bars. *ACI Mater. J.* **1998**, *95*, 609–616.
31. Malvar, L.J.; Crawford, J.E. *Dynamic Increase Factors for Concrete*; Naval Facilities Engineering Service Center: Port Hueneme, CA, USA, 1998.
32. Thomas, R.J.; Sorensen, A.D. Review of strain rate effects for UHPC in tension. *Constr. Build. Mater.* **2017**, *153*, 846–856. [CrossRef]
33. Li, R.-H.; Li, C.; Li, H.-N.; Yang, G.; Zhang, P. Improved estimation on seismic behavior of RC column members: A probabilistic method considering dynamic effect and structural parameter uncertainties. *Struct. Saf.* **2023**, *101*, 102308. [CrossRef]
34. Huang, H.; Burton, H.V. Classification of in-plane failure modes for reinforced concrete frames with infills using machine learning. *J. Build. Eng.* **2019**, *25*, 100767. [CrossRef]
35. Zhang, H.; Cheng, X.; Li, Y.; He, D.; Du, X. Rapid seismic damage state assessment of RC frames using machine learning methods. *J. Build. Eng.* **2023**, *65*, 105797. [CrossRef]
36. Mangalathu, S.; Hwang, S.H.; Choi, E.; Jeon, J.S. Rapid seismic damage evaluation of bridge portfolios using machine learning techniques. *Eng. Struct.* **2019**, *201*, 109785. [CrossRef]
37. Elwood, K.J. Modelling failures in existing reinforced concrete columns. *Can. J. Civ. Eng.* **2004**, *31*, 846–859. [CrossRef]

38. Dodd, L.; Restrepo-Posada, J. Model for predicting cyclic behavior of reinforcing steel. *J. Struct. Eng.* **1995**, *121*, 433–445. [CrossRef]
39. Dhakal, R.; Maekawa, K. Modeling of post-yield buckling of reinforcement. *J. Struct. Eng.* **2002**, *128*, 1139–1147. [CrossRef]
40. Mander, J.A.B.; Priestley, M.J.N. Theoretical Stress-Strain Model for Confined Concrete. *J. Struct. Eng.* **1988**, *114*, 1804–1826. [CrossRef]
41. Comite Euro-International Du Beton. *CEB-FIP Model Code 1990: Design Code*; Thomas Telford Publishing: Buffalo, NY, USA, 1993.
42. Li, M.; Li, H.N. Effects of strain rate on reinforced concrete structure under seismic loading. *Adv. Struct. Eng.* **2012**, *15*, 461–476. [CrossRef]
43. Vecchio, F.J.; Collins, M.P. The modified compression-field theory for reinforced concrete elements subjected to shear. *ACI J.* **1986**, *83*, 219–231.
44. Xinxin, L. *Bond Behavior of Reinforcement in Concrete under Lateral Pressure and Dynamic Loading*; Dalian University of Technology: Dalian, China, 2016.
45. Zhao, J.; Sritharan, S. Modeling of strain penetration effects in fiber-based analysis of reinforced concrete structures. *ACI Mater. J.* **2007**, *104*, 133.
46. Moridani, K.K.; Zarfam, P. Nonlinear analysis of reinforced concrete joints with bond-slip effect consideration in OpenSees. *Nonlinear Anal.* **2013**, *3*, 362–367.
47. Jeon, J.-S.; Lowes, L.N.; DesRoches, R.; Brilakis, I. Fragility curves for non-ductile reinforced concrete frames that exhibit different component response mechanisms. *Eng. Struct.* **2015**, *85*, 127–143. [CrossRef]
48. Haskett, M.; Oehlers, D.J.; Ali, M.M. Local and global bond characteristics of steel reinforcing bars. *Eng. Struct.* **2008**, *30*, 376–383. [CrossRef]
49. Breiman, L. Random Forests. *Mach. Learn.* **2001**, *45*, 5–32. [CrossRef]

Disclaimer/Publisher's Note: The statements, opinions and data contained in all publications are solely those of the individual author(s) and contributor(s) and not of MDPI and/or the editor(s). MDPI and/or the editor(s) disclaim responsibility for any injury to people or property resulting from any ideas, methods, instructions or products referred to in the content.